

Active Thermal Control of AC/DC Power Converter Considering Health Monitoring of Power Modules

Ali Moghassemi
Holcombe Department of Electrical
and Computer Engineering
Clemson University
Clemson, SC, USA
amoghas@clemson.edu

Gokhan Ozkan
Holcombe Department of Electrical
and Computer Engineering
Energy Innovation Center
Clemson University
Clemson, SC, USA
gokhano@clemson.edu

Christopher S. Edrington
Holcombe Department of Electrical
and Computer Engineering
Clemson University
Clemson, SC, USA
cedring@clemson.edu

Grace Muriithi
Automotive Engineering Department
Clemson University
Clemson, SC, USA
gmuriit@clemson.edu

Zheyu Zhang
Holcombe Department of Electrical
and Computer Engineering
Clemson University
Clemson, SC, USA
zheyuz@clemson.edu

Abstract—The evolution of power electronics devices in the semiconductor sector has created a strong need for power modules that have high efficiency and low power usage. The power package; which embraces a couple of power electronics devices such as switches and diodes; provides mechanical supports, electrical interface, protection, and thermal management to the power electronics devices. The power package is power dissipation, resulting in a significant challenge to its thermal management. To lower the expenses on wasted power and minimize the need for cooling systems, it is imperative for power converters and their control algorithm to offer exceptional efficiency in converting power. Hence, efficient thermal control and sophisticated thermal design are crucial in developing the power module. In this paper, health monitoring of the power modules is considered in the active thermal control of a two-level power rectifier using a sequence-based model predictive control method. This paper sets the stage for monitoring the thermal response and health of power electronics devices by early diagnosis of degradation. This declines the thermal stress and makes a prompt prediction of failure. This would enhance the reliability of the power converter.

Index Terms—Active Thermal Control, Health Monitoring, Degradation Diagnosis, Model Predictive Control, and Sequence-based Control.

I. INTRODUCTION

Power converters have a broad range of applications, including but not limited to renewable energy systems like solar photovoltaic systems [1] and wind turbines [2], electric vehicles and motor drives [3], and power custom devices [4]. Reliability for power converters has been a pressing issue as it is a decisive factor in the design of the power system [5], [6]. In order to increase power density and decrease material usage,

This material is based upon research supported by the US Office of Naval Research (ONR) under award number N00014-22-1-2558, and it is approved for public release under DCN# 543-100-23.

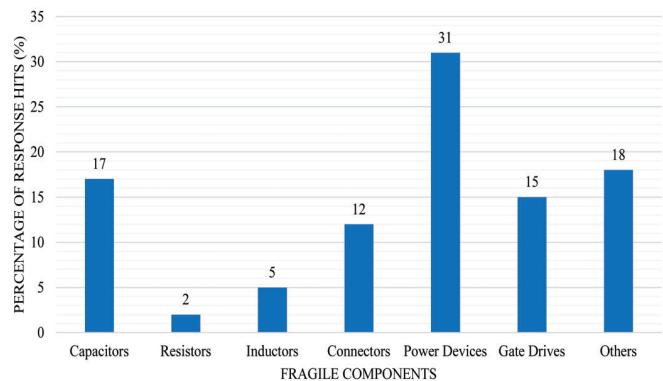


Fig. 1. Vulnerable elements

power semiconductor devices (PSD) are typically combined into modules [7]. Based on a survey conducted within the industry in [8], the PSDs were chosen by 31%

As previously mentioned, one can declare that The dependability of the PSDs is closely associated with the reliability of the power system. The failure of PSDs is the root cause of the fault in the power converter, meaning that improving the reliability of the PSDs leads to an increase in the power converter reliability. To tackle this concern, numerous studies have been done over the years, such as methods for estimating remaining useful lifetime (RUL), condition monitoring (CM), and active thermal control (ATC), as depicted in Figure 2. The theory behind the CM is to opt for a physical measurement, which demonstrates the occurrence of failures or degradation in the whole power system. The appropriate actions can then be taken per the outputs of the CM to avert an abrupt shutdown

of the system.

Another approach to enhance the reliability of the PSDs is the ATC. Figure 2 illustrates how the data on degradation indicators obtained through online CM methods can be used to update the system passively and even actively manage the system lifetime in conjunction with the ATC. As previously stated, PSD failures primarily occur due to thermal stress. The ATC can alleviate the thermal stress on components without altering the converter, either by lowering the temperature fluctuation amplitude or decreasing the average temperature. This means there probably be no additional expenses for improving the converter design or elements. It is worth pointing out that the thermal control capability and the power system's performance must be simultaneously considered. Finally, the RUL estimation method is, by and large, deployed to design the ATC and then validate its effect. Figure 2 shows the relationship between the CM, the ATC, and the RUL estimation methods.

The ATC approach addresses short-term and medium-term thermal cycles and adjusts the junction temperatures in real-time using temperature control parameters. The goal is to minimize thermal stress in the module by smoothing out temperature fluctuations. To influence the junction temperatures, thermal control adjusts the losses in the desired chips by increasing or decreasing them for a certain period. Over the past years, several techniques have been proposed for the ATC aspect of PSDs. The most important control parameters are the switching frequency [3] and [9], the modulation approach [10], the dc-link voltage [11], the gate voltage [12], or circulating reactive power [13]. For instance, a short-term temperature drop can be averted or decreased when losses are escalated temporarily by increasing the switching frequency. While CM necessitates understanding the junction temperature, ATC can function without such information [14]. Additionally, using an electrothermal model to derive real-time estimates of the junction temperatures through electrical measurements is possible, enabling more accurate management of thermal stress [3].

The most widely used control method in power converters is the linear control theory [15], [16]. However, it has some demerits and is unsuitable for all applications. A better solution that overcomes these issues is sequence-based control. It has been and is deployed in various applications, such

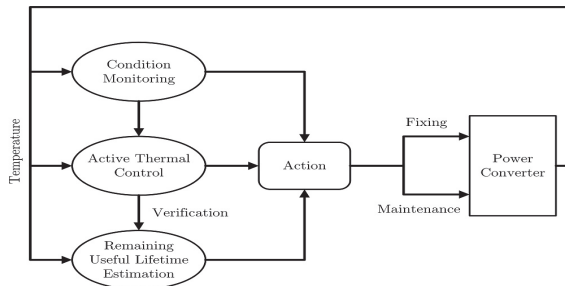


Fig. 2. Relationship between the CM, the ATC, and the RUL methods

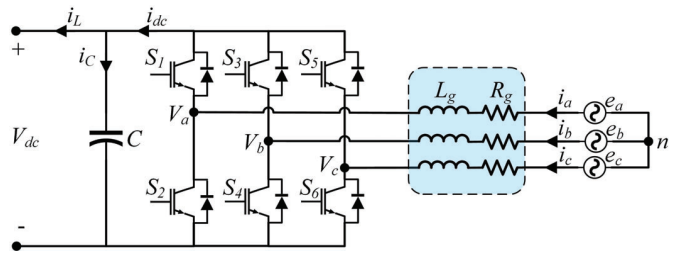


Fig. 3. The physical model of 2L3P power rectifier

as battery charging, renewable energy systems, and motor drives [17] - [21], to improve the effectiveness of the power converters regarding their reliability, efficiency, and thermal regulation. In this method, the mathematical model of the system is employed to estimate its controlled variables per a pre-defined prediction horizon. These variables are obtained from the cost function that tries to minimize the error for enhancement in the performance, like voltage and current total harmonic distortion (THD) values and thermal control over the switching stage. The sequence-based control outperforms the linear control approaches as the objective function in the sequence-based control encompasses several weighted multi-objective constraints.

This paper proposes the sequence-based control method to control an AC/DC power rectifier. This approach involves modifying the bus voltage while maintaining constant power usage and controlling the temperature of the PSDs. In order to accomplish this, both the electrical and thermal characteristics of the power converter are taken into account. Plus, a notional degradation of power modules has been considered for health monitoring of the power converter.

The rest of this work is organized in a following manner. Section II presents the control design of the sequence-based model predictive control, loss model, thermal model, and state-of-health model. Section III provides the simulation results and comparisons. The paper is finally concluded in section IV.

II. METHODOLOGY

A. Sequence-based Model Predictive Control

Generally, the sequence-based model predictive control method is based on a finite number of switching states of the power modules in the power electronics converter. Thus, the optimum switching state is required. For this purpose, it is necessary to have an objective function that can compute the difference between anticipated and desired values. Therefore, the switching state that has been selected (as it optimizes the objective function) is utilized for the subsequent time horizon. In addition to providing an optimal control strategy for each switching state, this approach also incorporates the non-linear thermal model into the control law. The illustration in Figure 3 depicts the physical model of a two-level three-phase (2L3P) power rectifier. This model is needed for the calculation of the predicted values.

In this figure, L_g is filter inductance, R_g is filter resistance, $S_1, S_3,$ and S_5 are upper switches in the legs, $S_2, S_4,$ and S_5 are lower switches in the legs, $i_{dc}, i_C,$ and i_L are DC output current, capacitor current, and load current, respectively. Finally, V_{dc} is the DC voltage.

Considering Kirchhoff's voltage law (KVL) results in the following equations:

$$L_g \frac{di_a(t)}{dt} + R_g i_a(t) + v_a(t) - e_a(t) = 0 \quad (1)$$

$$L_g \frac{di_b(t)}{dt} + R_g i_b(t) + v_b(t) - e_b(t) = 0 \quad (2)$$

$$L_g \frac{di_c(t)}{dt} + R_g i_c(t) + v_c(t) - e_c(t) = 0 \quad (3)$$

Note that (1)-(3) are continuous-time equations that increase the computational burden. Therefore, a discretization conversion is of the essence. There are several discretization approaches, like forward Euler, backward Euler, and midpoint, each of which can serve the purpose, but they have their own merits and demerits. In this work, the forward Euler method is chosen for its simplicity and offering good precision. Equation (4) expresses the conversion of (1)-(3) into the discrete-time equation with one prediction horizon:

$$L_g \left(\frac{i(k+1) - i(k)}{T_s} \right) + v(k) + R_g i(k) - e(k) = 0 \quad (4)$$

In which T_s is the sampling period of the discretization. As a result, the predicted current in (4) can also be written more simply as follows:

$$i(k+1) = \frac{T_s}{L_g} \left(e(k) - v(k) - R_g i(k) \right) + i(k) \quad (5)$$

Based on this equation and all possible switching states (which are eight for the 2L3P power rectifier), voltage vectors, as depicted in Figure 4, are achieved.

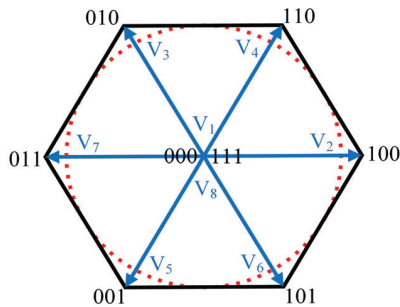


Fig. 4. Voltage vectors and switching states for 2L3P power rectifier

B. Loss Model

The chief losses associated with power converters are switching losses and conduction losses. Ref. [5] provides a rough calculation of the dependency of the switching energy dissipation for the IGBT and the diode:

$$E_{sw} = E_{swref} \left(\frac{i_c}{i_{ref}} \right)^{K_i} \left(\frac{v_{dc}}{v_{ref}} \right)^{K_v} \left(1 + TC_{sw}(T_j - T_{jref}) \right) \quad (6)$$

In (6), $E_{sw} = E_{on} + E_{off}$ for the IGBT and $E_{sw} = E_{rr}$ for the free wheeling diode. E_{on} and E_{off} are IGBT switching energy, and E_{rr} is diode recovery energy. $i_{ref}, v_{ref},$ and T_j are reference current, voltage, and junction temperature obtained from the power module's datasheet or manual, respectively. K_i and K_v are exponent of current and voltage dependencies, and TC_{sw} is temperature coefficient of switching losses. Considering (6) for the IGBT and the diode, (7) and (8) express the calculation of the two major losses (conduction and switching losses):

$$P_{sw,loss} = \left(\frac{E_{sw,igbt} + E_{sw,diode}}{T_s} \right) \quad (7)$$

$$P_{c,loss} = \left(\frac{E_{c,igbt} + E_{c,diode}}{T_s} \right) \quad (8)$$

Therefore, the total power losses on the PSDs can be presented as follows:

$$P_{loss} = P_{sw,loss} + P_{c,loss} \quad (9)$$

The above equations provide a reliable estimate of the power losses of the PSDs. This paper includes an error regarding the degradation of the PSDs for monitoring their health status. This will be explained more in Subsection D of Section II.

C. Thermal Model

The thermal feature of the power converters is expressed with several thermal resistors and capacitors, as explained in [22]. It should be noted that the only factors taken into account by the thermal model in predicting junction temperature are the ambient temperature and power losses, which lead to thermal cycling. Although this temperature alters slowly in almost all applications, changes in power losses are highly operating-point dependent. This paper uses the Cauer thermal network to model the PSDs' thermal feature, as depicted in Figure 5.

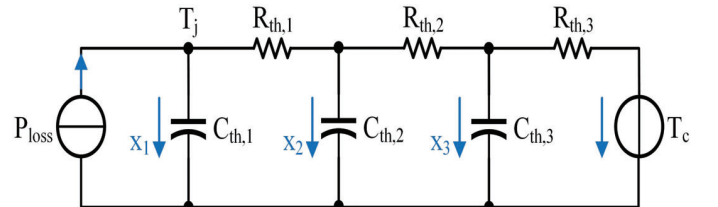


Fig. 5. The Cauer thermal network for the 2L3P power rectifier

Considering Kirchhoff's current law (KCL) to the thermal model, the state equations (10)-(12) are achieved:

$$\frac{dx_1}{dt} = -\frac{1}{C_{th,1}R_{th,1}}x_1 + \frac{1}{C_{th,1}R_{th,1}}x_2 + \frac{1}{C_{th,1}}P_{loss}(t) \quad (10)$$

$$\frac{dx_2}{dt} = \frac{1}{C_{th,2}R_{th,1}}x_1 - \frac{R_{th,1} + R_{th,2}}{C_{th,2}R_{th,1}R_{th,2}}x_2 + \frac{1}{C_{th,2}R_{th,2}}x_3 \quad (11)$$

$$\frac{dx_3}{dt} = \frac{1}{C_{th,3}R_{th,2}}x_2 - \frac{R_{th,2} + R_{th,3}}{C_{th,3}R_{th,2}R_{th,3}}x_3 + \frac{1}{C_{th,3}R_{th,3}}T_c(t) \quad (12)$$

Here, x_1 to x_3 represent the temperature amounts of the thermal capacitors, and T_c is the ambient temperature.

D. State-of-Health (SoH) Diagnosis

To monitor the health status of the PSDs, variations in power losses can account for the behavior of the power modules. The estimation of this error in the predicted power losses will be monitored throughout the PSDs' lifetime, thus diagnosing their behavior as early critical degradation. Figure 6 shows the model for the power losses during the operation through the lifetime of the power converter. As is evident, the rise in power losses after operating the PSD for a long time is considered to diagnose worn-out status or degradation of the PSDs associated with their electrical or thermal response. The obtained failure indicators provide the early SoH diagnosis so that the required actions for maintenance or substitution are taken. This is of the utmost importance to enhance the reliability and availability of the PSDs and the power converter throughout their lifetime. In this paper, a notional degradation for the power module is considered to assess the effectiveness of the control method when one of the power modules begins to wear out. One way to model the degradation of a PSD is to vary the thermal resistance. An alternative method involves determining the thermal impedances of the PSDs through in-situ thermal impedance spectroscopy (ITIS). This approach allows for evaluating the PSD's thermal impedance across various frequency ranges while the converter operates normally.

Thermal cycle tests under periodic loading will be conducted to analyze the experimental degradation and end-of-life estimation. By deducing the data acquired from these tests, empirical aging models can be achieved that calculate the number of cycles to failure as a function of the temperature

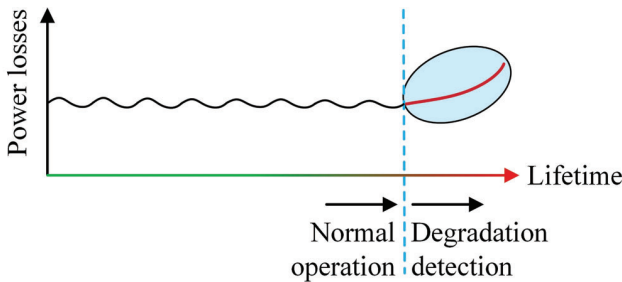


Fig. 6. Power loss model and degradation detection for the power converter or the power modules

cycle and the operating conditions. It should be noted that in order to determine when a power module has reached the end of its useful life, instead of observing the real-time failure, specific thresholds for failure indicators that provide a clear definition of the module's end-of-life must be established. When these thresholds are surpassed, the power module may still function, but its degradation has progressed to a point where its reliability cannot be assured for continued operation under extreme conditions.

In Figure 7, there is an illustration of the various stages and durations involved in monitoring the health of a system and predicting its lifetime events [23]. To begin, it is necessary to define the upper failure threshold, lower failure threshold, upper threshold, and lower threshold values. Within this diagram, t_0 represents the moment when the system is powered on, while t_E signifies the occurrence of an off-nominal event. Off-nominal events happen when the measured variable exceeds the threshold values. A prognostics and health management (PHM) system detects such an event at t_D . Subsequently, the PHM system computes the anticipated failure time of the system. The response time, denoted as t_R , corresponds to the duration taken by the PHM system to generate a predicted failure time and provide a useful prediction at time t_P . Finally, t_F indicates the actual time when the system experiences a failure.

The thermal observer configurations enable the calculation of degradation indicators that help identify when the power module undergoes changes in its electrothermal behavior. These indicators can be conveniently computed in real-time using data about the junction temperature, which can be acquired through temperature sensors or temperature-sensitive electrical parameters (TSEPs) methods. An accurate estimation of the average power loss is crucial for observing the degradation. Any changes observed in the power loss throughout the converter operation often indicate degradation mechanisms. Additionally, reliable measurement of the cooling part of the converter, achieved through sensors, is essential for precise thermal monitoring during experimental degradation analysis.

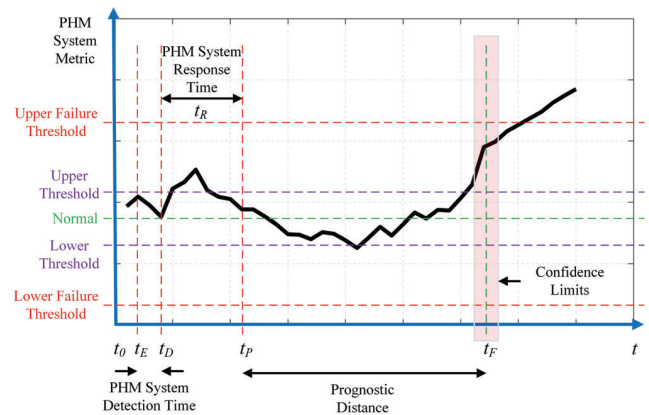


Fig. 7. The pathway of a system's failure

During real-time operation, the ATC method can effectively regulate the rate at which the PSDs degrade by preventing excessive temperatures and minimizing power cycling. As a result, thermal stress is reduced, decreasing the overall degradation of the PSDs.

E. Cost Function

The critical point in the cost function is to address one or multiple problems simultaneously, considering all the constraints and restrictions of the issues. In this paper, the main two objectives are the ATC of the PSDs and control of the DC-link voltage. For the thermal aspect of the PSDs, the cost function that minimizes the difference between the predicted and the reference junction temperature values must be considered as follows:

$$OF_T = |T_j^*(k+1) - T_j(k+1)| \quad (13)$$

For controlling the DC-link voltage, the cost function should be expressed as follows:

$$OF_E = |i_\alpha^*(k+1) - i_\alpha(k+1)| + |i_\beta^*(k+1) - i_\beta(k+1)| \quad (14)$$

In (14), the superscripts denoted by asterisks correspond to the current reference values for the following time period. In contrast, those without asterisks correspond to the projected current values for a specific voltage vector.

Equation (15) expresses the cost function that includes the electrical term for the DC-link voltage control and the ATC of the PSDs:

$$OF_{ET} = \omega_T OF_T + \omega_E OF_E \quad (15)$$

$$\omega_T + \omega_E = 1 \quad (16)$$

In this equation, ω_T and ω_E are the weight factors for thermal and DC-link voltage terms, respectively.

III. SIMULATION RESULTS

Figure 8 illustrates the electrothermal control scheme that includes the physical and control systems in which the electrical and thermal models are shown. As can be observed in this figure, the values of the AC voltage (e_{abc}), the AC current (i_{abc}), the rectifier DC voltage (v_{dc}), and the ambient temperature (T_c) are calculated from the physical model. The DC voltage is adjusted to produce the current reference value. As described in equation (15), the objective function, which minimizes the discrepancies in the electrical term for DC-link voltage control and ATC of the PSDs, generates the most effective switching signals for the power rectifier. Regarding monitoring the state-of-health (SoH) of the PSDs, if the difference between the measured power losses surpasses a predetermined threshold, it indicates a reliable sign of the PSDs' degradation and their SoH. The obtained data from the SoH will be of considerable importance for early diagnosis of health conditions of the PSDs and maintenance and/or replacement ahead of schedule since it provides information about their degradation due to thermal stress.

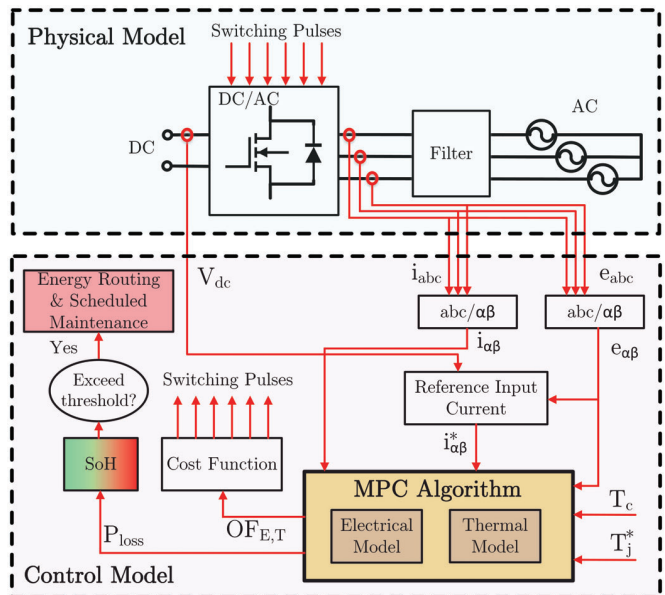


Fig. 8. Power loss model and degradation detection for the power converter or the power modules

TABLE I
MODEL PARAMETERS

Parameters	Values
AC Line-to-line Voltage (e_{abc})	480 V
Frequency (f)	60 Hz
Rectifier Rated Power (P)	20 kW
DC-link Voltage (V_{dc})	800 V
Control Sampling Time (T_c)	100 μ s
Simulation Step Time (T_s)	5 μ s
DC-link Capacitor (C)	940 μ F
Grid Filter Inductance (L_g)	7 mH
Grid Filter Resistance (R_g)	0.005 Ω

The models are simulated in the MATLAB/Simulink platform. The simulation model parameters are outlined in Table I. The proposed system is studied under normal and unhealthy conditions in this section.

A. Normal Conditions

In this section, the simulation is carried out with different weight factors (ω_E) to analyze the performance of the proposed control system when the ambient temperature is set to 25°C. It is worth stressing again that the sequence-based active thermal control method aims to achieve the optimal switching status, thereby reducing thermal stress across the PSDs by reducing the temperature and the power losses. The performance of the control system is demonstrated in Figures 9, 10, and 11 for various ω_E values, namely $\omega_E=0.2$ (with thermal control), $\omega_E=0.5$ (with thermal control), and $\omega_E=1$ (without thermal control). Table II summarizes the control system's outcomes in current THD, voltage THD, median power loss, and median junction temperature.

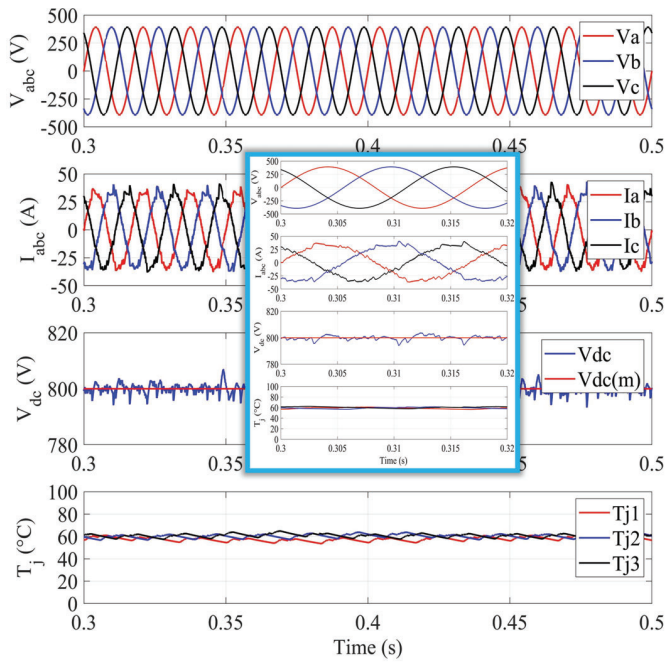


Fig. 9. The effect of $\omega_E=0.2$ (with thermal control) on the control system's performance

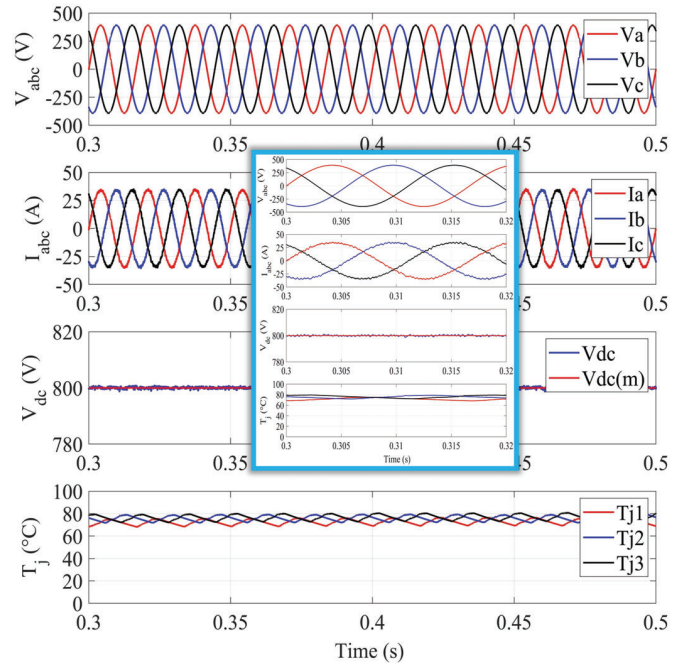


Fig. 11. The effect of $\omega_E=1$ (without thermal control) on the control system's performance

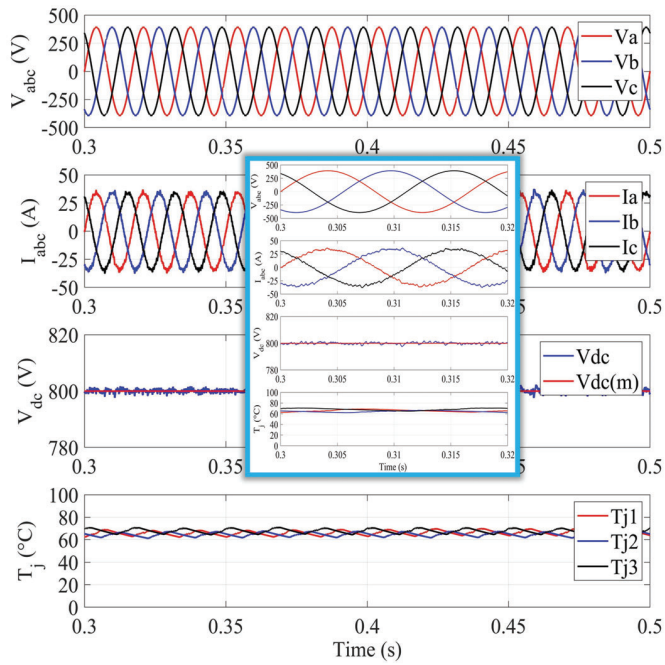


Fig. 10. The effect of $\omega_E=0.5$ (with thermal control) on the control system's performance

As can be seen in Figures 9-11 and Table II, the current THD and the DC-link voltage ripple decrease as ω_E increases. On the other hand, the power losses decline as ω_E decreases. This poses a dilemma between power loss reduction to improve the power rectifier's efficiency and current THD

TABLE II
MODEL PARAMETERS

Weight Factor ω_E (%)	Current THD THD_i (%)	Power Loss P_{loss} (W)	Junction Temperature T_j (°C)
100	2.94	431.3	78.84
90	3.43	425.7	77.83
80	4.32	419.0	77.18
70	5.44	410.8	76.41
60	6.78	388.7	74.05
50	8.90	347.3	69.56
40	12.03	322.1	66.75
30	16.33	295.66	64.32
20	27.81	287.04	63.73

reduction to enhance the power rectifier's power quality.

B. Degradation Conditions

In this section, a notional degradation for the power module is taken into account two times, between $1.3s < t < 0.301s$ and $1.8s < t < 1.804s$ to monitor the performance of the control method when one of the power modules begins to wear out.

To this end, as illustrated in Figure 12, if the power losses are within the pre-defined threshold, no degradation is detected, and the power converter keeps operating. If the difference between the measured power losses surpasses a predetermined threshold, it indicates a dependable sign of the PSDs' degradation and their SoH. As can be seen, the temperature increases as the power losses increase, meaning that degradation is going to happen. With this feature, future monitoring systems can achieve information regarding the

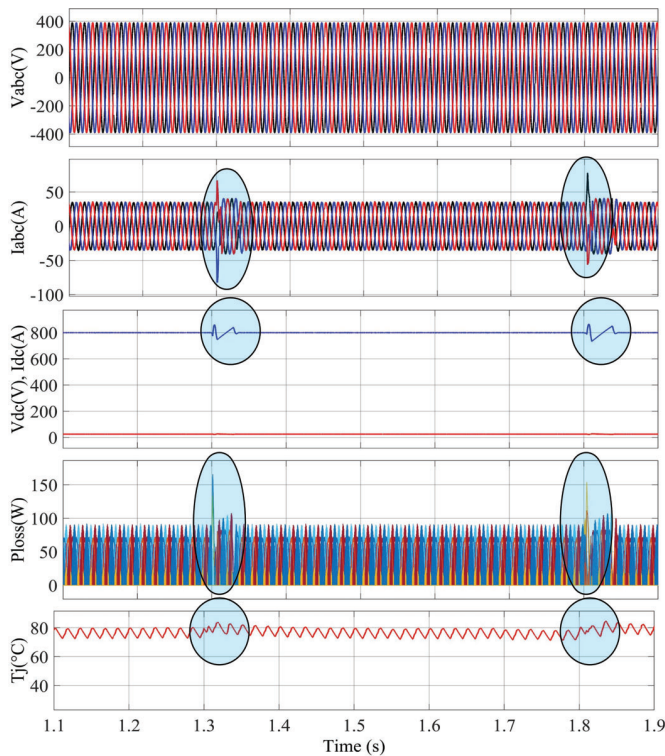


Fig. 12. Degradation and SoH of the power converter

thermal response and degradation, thereby securing the PSDs from intense thermal stress and overload.

The data obtained from the SoH, as shown in Figure 8, will be of considerable importance for early diagnosis of health conditions of the PSDs and maintenance and/or replacement ahead of schedule since it provides information about their degradation due to thermal stress. Early degradation diagnosis and the SoH of the power converter bring benefits, such as lower maintenance times and lower degradation effect on healthy PSDs.

By utilizing these advanced capabilities, future monitoring systems can obtain thermal feedback and detect degradation, resulting in enhanced protection of power modules from excessive thermal strain and overload.

Aside from this, one decisive approach is called energy or power routing. This method - which is more prevalent in multi-level power converters or power electronics building blocks (PEBB) concept - distributes power between the modular power electronics converter cells to reduce their thermal stress, thus increasing their lifetime.

IV. CONCLUSION

This paper presents the sequence-based active thermal control of the 2L3P power rectifier. The simulation outcomes indicate that the suggested control technique can diminish power losses and regulate the power module's junction temperature. This leads to efficiency enhancement and reduction in the required cooling system, especially in the shipboard

electric power systems where many power converters operate simultaneously. Despite the reduction in power losses, there is an increase in both the current THD values and the ripple of the DC-link voltage. Selecting the optimal weight factor is a difficult task as it must satisfy the power converter's electrical and thermal demands. Also, when the degradation of the power modules happens, their health status must be monitored to take required and urgent actions. The control method presented in this study can promptly detect power module degradation by identifying errors in the electrothermal model and changes in power losses resulting from degradation.

Future research will concentrate on the health monitoring and lifetime forecasting of the PEBBs concept, which involves more complex physical models, thermal models, and control systems. The improved lifetime will lower the costs regarding maintenance and materials due to lower replacement elements.

ACKNOWLEDGMENT

This material is based upon research supported by the US Office of Naval Research (ONR) under award number N00014-22-1-2558, and it is approved for public release under DCN# 543-100-23.

REFERENCES

- [1] A. Moghasssemi, D.S. Vanaja, J. Olamaei, G. Ozkan and C.S. Edrington, "A Novel Switching Method in PV-fed Quasi-ZSI-DVR For Voltage Quality Enhancement of Photovoltaic Integrated Networks," *IET Renewable Power Generation*. 2022, doi: 10.1049/rpg2.12575.
- [2] F. Blaabjerg and K. Ma, "Future on Power Electronics for Wind Turbine Systems," *IEEE Journal of Emerging and Selected Topics in Power Electronics*, vol. 1, no. 3, pp. 139-152, 2013, doi: 10.1109/JESTPE.2013.2275978.
- [3] J. Lemmens, P. Vanassche and J. Driesen, "Optimal Control of Traction Motor Drives Under Electrothermal Constraints," *IEEE Journal of Emerging and Selected Topics in Power Electronics*, vol. 2, no. 2, pp. 249-263, 2014, doi: 10.1109/JESTPE.2014.2299765.
- [4] A. Moghasssemi and S. Padmanaban, "Dynamic Voltage Restorer (DVR): A Comprehensive Review of Topologies, Power Converters, Control Methods, and Modified Configurations," *Energies*, vol. 13, no. 16, p. 4152, 2020, doi: 10.3390/en13164152.
- [5] H. Wang, M. Liserre and F. Blaabjerg, "Toward Reliable Power Electronics: Challenges, Design Tools, and Opportunities," *IEEE Industrial Electronics Magazine*, vol. 7, no. 2, pp. 17-26, 2013, doi: 10.1109/MIE.2013.2252958.
- [6] H. Wang et al., "Transitioning to Physics-of-Failure as a Reliability Driver in Power Electronics," *IEEE Journal of Emerging and Selected Topics in Power Electronics*, vol. 2, no. 1, pp. 97-114, 2014, doi: 10.1109/JESTPE.2013.2290282.
- [7] Power Semiconductors, *Application Manual Power Semiconductors*, SEMIKRON International GmbH, Nuremberg, Germany, 2010. Available online: <https://www.semikron-danfoss.com/service-support/application-manual.html>
- [8] S. Yang, A. Bryant, P. Mawby, D. Xiang, L. Ran and P. Tavner, "An Industry-Based Survey of Reliability in Power Electronic Converters," *IEEE Transactions on Industry Applications*, vol. 47, no. 3, pp. 1441-1451, 2011, doi: 10.1109/ECCE.2009.5316356.
- [9] D. A. Murdock, J. E. R. Torres, J. J. Connors and R. D. Lorenz, "Active Thermal Control of Power Electronic Modules," *IEEE Transactions on Industry Applications*, vol. 42, no. 2, pp. 552-558, 2006, doi: 10.1109/TIA.2005.863905.
- [10] M. Weckert and J. Roth-Stielow, "Lifetime As A Control Variable in Power Electronic Systems," in *2010 Emobility - Electrical Power Train*, 2010, pp. 1-6, doi: 10.1109/EMOBILITY.2010.5668049.
- [11] J. Lemmens, J. Driesen and P. Vanassche, "Dynamic DC-link Voltage Adaptation For Thermal Management of Traction Drives," in *2013 IEEE Energy Conversion Congress and Exposition*, 2013, pp. 180-187, doi: 10.1109/ECCE.2013.6646698.

- [12] C. Sintamarean, H. Wang, F. Blaabjerg and F. Iannuzzo, "The Impact of Gate-driver Parameters Variation and Device Degradation in the PV-inverter Lifetime," in *2014 IEEE Energy Conversion Congress and Exposition (ECCE)*, 2014, doi: 10.1109/ECCE.2014.6953704.
- [13] K. Ma, M. Liserre and F. Blaabjerg, "Reactive Power Influence on the Thermal Cycling of Multi-MW Wind Power Inverter," *IEEE Transactions on Industry Applications*, vol. 49, no. 2, pp. 922-930, 2013, doi: 10.1109/TIA.2013.2240644.
- [14] M. Andresen, G. Buticchi, J. Falck, M. Liserre and O. Muehlfeld, "Active Thermal Management For A Single-phase H-Bridge Inverter Employing Switching Frequency Control," in *Proceedings of PCIM Europe 2015; International Exhibition and Conference for Power Electronics, Intelligent Motion, Renewable Energy and Energy Management*, 2015, pp. 1-8.
- [15] N. Mohan, T. M. Undeland and W. P. Robbins, *Power Electronics; Converters, Applications and Design*, Hoboken, New Jersey, USA: John Wiley & Sons, 2007.
- [16] M. H. Rashid, *Power Electronics Handbook*, 4th. ed., Oxford, United Kingdom: Butterworth-Heinemann, Elsevier, 2018, doi: 10.1016/C2016-0-00847-1.
- [17] M. Parvez, S. Mekhilef, N. M. L. Tan and H. Akagi, "Model Predictive Control of A Bidirectional AC-DC Converter For V2G and G2V Applications in Electric Vehicle Battery Charger," in *2014 IEEE Transportation Electrification Conference and Expo (ITEC)*, 2014, pp. 1-6, doi: 10.1109/ITEC.2014.6861795.
- [18] B. Feng and H. Lin, "Finite Control Set Model Predictive Control of AC/DC Matrix Converter for Grid-Connected Battery Energy Storage Application," *Journal of Power Electronics*, vol. 15, no. 4, pp. 1006-1017, 2015, doi: 10.6113/JPE.2015.15.4.1006.
- [19] P. Karamanakos, E. Liegmann, T. Geyer and R. Kennel, "Model Predictive Control of Power Electronic Systems: Methods, Results, and Challenges," *IEEE Open Journal of Industry Applications*, vol. 1, pp. 95-114, 2020, doi: 10.1109/OJIA.2020.3020184.
- [20] W. Razia Sultana, Sarat Kumar Sahoo, Sukruedee Sukchai, S. Yamuna and D. Venkatesh, "A Review on State of Art Development of Model Predictive Control for Renewable Energy Applications," *Renewable and Sustainable Energy Reviews*, vol. 76, pp. 391-406, 2017, doi: 10.1016/j.rser.2017.03.058.
- [21] M. Khalilzadeh, S. Vaez-Zadeh, J. Rodriguez and R. Heydari, "Model-Free Predictive Control of Motor Drives and Power Converters: A Review," *IEEE Access*, vol. 9, pp. 105733-105747, 2021, doi: 10.1109/ACCESS.2021.3098946.
- [22] J. Falck, M. Andresen and M. Liserre, "Active thermal control of IGBT power electronic converters," in *IECON 2015 - 41st Annual Conference of the IEEE Industrial Electronics Society*, 2015, pp. 000001-000006, doi: 10.1109/IECON.2015.7392925.
- [23] *IEEE Standard Framework for Prognostics and Health Management of Electronic Systems*. IEEE Standard 1856-2017, 2017, doi: 10.1109/IEEESTD.2017.8227036.